HHS Public Access

Author manuscript

Glia. Author manuscript; available in PMC 2016 December 04.

Published in final edited form as:

Glia. 2015 November ; 63(11): 1982–1996. doi:10.1002/glia.22868.

Chronic reactive gliosis following regulatory T cell depletion during acute MCMV encephalitis

James R. Lokensgard, **Scott J. Schachtele**, **Manohar B. Mutnal**, **Wen S. Sheng**, **Sujata Prasad**, and **Shuxian Hu**

University of Minnesota, Center for Infectious Diseases and Microbiology Translational Research, Department of Medicine, 3-140 McGuire Translational Research Facility, 2001 6th St. SE, Minneapolis, MN, USA

Abstract

Long-term, persistent central nervous system inflammation is commonly seen following brain infection. Using a murine model of viral encephalitis (murine cytomegalovirus, MCMV) we have previously shown that post-encephalitic brains are maintained in an inflammatory state consisting of glial cell reactivity, retention of brain-infiltrating tissue-resident memory $CD8^+$ T-cells, and long-term persistence of antibody-producing cells of the B-lineage. Here, we report that this neuroinflammation occurs concomitantly with accumulation and retention of immunosuppressive regulatory T-cells (Tregs), and is exacerbated following their ablation. However, the extent to which these Tregs function to control neuroimmune activation following MCMV encephalitis is unknown. In this study, we used Foxp3-diphtheria toxin receptor-GFP (Foxp3-DTR-GFP) transgenic mice, which upon administration of low-dose diphtheria toxin (DTx) results in the specific depletion of Tregs, to investigate their function. We found treatment with DTx during the acute phase of viral brain infection (0 – 4 dpi) resulted in depletion of Tregs from the brain, exacerbation of encephalitis (i.e., increased presence of $CD4^+$ and $CD8^+$ T-cells), and chronic reactive phenotypes of resident glial cells (i.e., elevated MHC class II as well as PD-L1 levels, sustained microgliosis, and increased glial fibrillary acidic protein (GFAP) expression on astrocytes) vs. untreated, infected animals. This chronic proinflammatory environment was associated with reduced cognitive performance in spatial learning and memory tasks (Barnes Maze) by convalescent animals. These data demonstrate that chronic glial cell activation, unremitting post-encephalitic neuroinflammation, and its associated long-term neurological sequelae in response to viral brain infection are modulated by the immunoregulatory properties of Tregs.

Keywords

microglia; astrocyte; reactive gliosis; Tregs; Foxp3; MCMV; encephalitis

Corresponding author: James R. Lokensgard, 3-220 McGuire Translational Research Facility, 2001 6th St. SE, Minneapolis, MN, USA, loken006@umn.edu, ph #: 612-626-9914.

Introduction

Long-term, persistent inflammation of the central nervous system (CNS) is commonly seen following viral brain infection (Neumann 2001). Evidence suggests that even after clearance of detectable viral antigen and resolution of acute inflammation, the brain does not immediately return to its pre-infection condition, but rather is maintained for a prolonged period in a chronic, heightened proinflammatory state. Using well-established herpes simplex virus (HSV)-1 and murine cytomegalovirus (MCMV) experimental brain infection models, our previous studies have shown that microglia, identified as $CD45^{int}CD11b^{+}$ cells residing within the brain, do not acquire reactive phenotypes solely do to innate responses to viral proteins themselves. Following brain infection, the vast majority of microglia display chronic reactivity, even in areas distal to viral replication. Rather, glial cells residing within the brain react to adaptive immune responses and mediators produced by brain-infiltrating T-cells, including interferon (IFN)-γ (Marques et al. 2008; Mutnal et al. 2011). In addition to viral infection, prolonged activation of resident microglia, along with sustained presence of brain resident memory T-cells, has been demonstrated in a wide variety of neurodegenerative diseases, CNS insults, and stroke, reviewed in (Burda and Sofroniew 2014).

Properly regulated neuroimmune responses to infection must strike a balance between pathogen clearance and an acceptable level of bystander tissue damage. Prolonged immune responses within the brain following MCMV infection are characterized by persistence of antibody-producing B-cells, chronic microglial cell activation, and retention of virus-specific effector-memory $CD8^{+}$ T-cells (Mutnal et al. 2011; Mutnal et al. 2012). Although $CD8^{+}$ T-cells play a critical role in controlling viral spread during acute brain infection (Cheeran et al. 2005; Reddehase et al. 1987), the chronic presence of these IFN-γ-producing lymphocytes may be damaging to the brain. In addition to the beneficial, antiviral effects of turning on proinflammatory neuroimmune responses, suppression of inflammation is equally critical to limiting tissue damage and preserving neurological function.

Our laboratory has been investigating various processes by which tissue-damaging inflammatory responses are controlled following viral brain infection. We have recently shown that both microglial cells and astrocytes possess the ability to suppress post-encephalitic $CD8^{+}$ T lymphocytes through up-regulation of a ligand for the programmed death receptor (PD)-1 (i.e., programmed death ligand 1, PD-L1, B7-H1, CD274), (Schachtele et al. 2014). Additional studies have demonstrated that anti-inflammatory, interleukin (IL)-10-producing regulatory B-cells (B10) which modulate microglial cell, as well as T lymphocyte, responses are found within post-encephalitic brains (Mutnal et al. 2014). Cytotoxic $CD8^{+}$ T-cells have been shown responsible for the destruction of healthy bystander neurons (McPherson et al. 2006). While maintaining a heightened state of immune readiness following viral infection may promote protection and lead to more rapid pathogen clearance following re-exposure or reactivation, it is clear that these chronic responses also need to be well-regulated.

It has been well-established that $CD4^{+}$ regulatory T-cells (Tregs) maintain order during autoimmune and inflammatory responses, as well as immune responses generated during viral infection (Lanteri et al. 2009; Suvas et al. 2004; Trandem et al. 2010). In addition,

Tregs are required to minimize tissue damage in response to viral infection, reviewed in (Veiga-Parga et al. 2013), and imbalance or dysfunction caused by depletion of the Treg population during viral infection has been demonstrated to lead to pathological tissue damage (Veiga-Parga et al. 2012). In addition, Treg depletion has been demonstrated to convert non-lethal encephalitis to one of high mortality, without affecting viral clearance (Anghelina et al. 2009). The presence of these cells has been reported within the brain following viral encephalitis, where their production of transforming growth factor (TGF)-β may support the maintenance of CNS-resident $CD8^+$ memory T-cells through increased CD103 expression (Graham et al. 2014). Recently, mouse hepatitis virus (MHV)-specific $Foxp3^+CD4^+$ Tregs have been detected within infected brains and been shown to ameliorate viral encephalitis by repressing effector T-cell function during both priming in the draining lymph nodes and effector stages (Zhao et al. 2014). These pathogen-specific Tregs were also demonstrated to diminish microglial cell activation during acute infection, as indicated by reduced expression of major histocompatibility complex (MHC) class II at 7 days post-infection (dpi) (Zhao et al. 2014). However, the full extent by which Tregs interact with resident brain cells to modulate viral encephalitis remains unknown. In this study, we investigated contributions of the Treg lymphocyte population in controlling reactive gliosis, along with post-encephalitic neuroinflammation and long-term neurological sequelae, at chronic time points post-infection.

Materials and Methods

Ethical statement

This study was carried out in strict accordance with recommendations in the Guide for the Care and Use of Laboratory Animals of the National Institutes of Health. The protocol was approved by the Institutional Animal Care and Use Committee (Protocol Number: 1402-31338A) of the University of Minnesota. All surgery was performed under Ketamine anesthesia and all efforts were made to minimize suffering.

Virus and animals

RM461, a MCMV expressing *Escherichia coli* β-galactosidase under the control of the human ie1/ie2 promoter/enhancer (Stoddart et al. 1994) was kindly provided by Edward S. Mocarski (Emory University, Atlanta, GA). The virus was maintained by passage in weanling female Balb/c mice (Charles River, Wilmington, MA). Salivary gland-passed virus was then grown in NIH 3T3 cells for 2 passages, which minimized any carry-over of salivary gland tissue. Infected 3T3 cultures were harvested at 80% to 100% cytopathic effect and subjected to three freeze–thaw cycles. Cellular debris was removed by centrifugation (1000 ×g) at 4°C, and the virus was pelleted through a 35% sucrose cushion (in Tris-buffered saline, 50 mM Tris–HCl, 150 mM NaCl, pH 7.4) at 23,000 ×g for 2 h at 4 °C. The pellet was suspended in Tris-buffered saline containing 10% heat-inactivated fetal bovine serum (FBS). Viral stock titers were determined on 3T3 cells as 50% tissue culture infective doses ($TCID_{50}$) per milliliter. Foxp3-GFP (Fontenot et al. 2005), as well as Foxp3-DTR-GFP (Kim et al. 2007), transgenic mice, each backcrossed over 15 generations onto the C57B/6 background (Ertelt et al. 2011), were kindly provided by Sing Sing Way (Cincinnati

Children's Hospital, Cincinnati, OH). Wild type C57B/6 mice were obtained from the Jackson Laboratories (Bar Harbor, ME).

Intracerebroventricular infection of mice

Infection of mice with MCMV was performed as previously described (Cheeran et al. 2004). Briefly, female mice (6–8 week old) were anesthetized using a combination of Ketamine and Xylazine (100 mg and 10 mg/kg body weight, respectively) and immobilized on a small animal stereotactic instrument equipped with a Cunningham mouse adapter (Stoelting Co., Wood Dale, IL). The skin and underlying connective tissue were reflected to expose reference sutures (sagittal and coronal) on the skull. The sagittal plane was adjusted such that bregma and lambda were positioned at the same coordinates on the vertical plane. Virulent, salivary gland-passaged MCMV RM461 (1×10^4 $TCID_{50}$ units in 10 μl), was injected into the right lateral ventricle at 0.9 mm lateral, 0.5 mm caudal, and 3.0 mm ventral to bregma using a Hamilton syringe (10 μl) fitted to a 27 G needle. The injection was delivered over a period of 3–5 min. The opening in the skull was sealed with bone wax and the skin was closed using 4-0 silk sutures with a FS-2 needle (Ethicon).

Regulatory T-cell depletion

Transgenic Foxp3-DTR-GFP mice were used to investigate the effects of acute Treg depletion on chronic neuroinflammation following viral encephalitis. Diphtheria toxin (DTx, Sigma-Aldrich, St. Louis, MO) stock solution was diluted to a concentration of either 0.5 μg/100μl or 0.1 μg/100μl. On the day prior to intracerebroventricular viral infection, a subset of mice were given intraperitoneal (ip) injections of DTx (0.5 μg/100μl). Subsequent doses of 0.1μg/100μl were given at 1 and 4 dpi to maintain Treg depletion throughout the acute phase of viral infection.

Isolation of brain leukocytes and FACS

Leukocytes were isolated from the brains of control C57B/6 mice as well as MCMV-infected mice with or without DTx treatment using a previously described procedure with minor modifications (Cheeran et al. 2007; Ford et al. 1995; Marten et al. 2003). In brief, whole brains were harvested, pooled (n = 4–6 animals/group/experiment), and minced finely in RPMI 1640 (2 g/L D-glucose and 10 mM HEPES) and digested in 0.0625% trypsin (in Ca/Mg-free HBSS) at room temperature for 20 min. Single cell preparations from the brains were suspended in 30% Percoll and banded on a 70% Percoll cushion at 900 ×g at 4°C for 15 min. Brain leukocytes obtained from the 30–70% Percoll interface were collected and used either for subsequent antibody staining for flow cytometry, or suspended in RPMI for *ex vivo* culture experiments. For flow cytometric antibody staining, brain leukocytes were first treated with Fc block (anti-CD32/CD16 in the form of 2.4G2 hybridoma culture supernatant with 2% normal rat and 2% normal mouse serum) to inhibit nonspecific Ab binding and were stained with anti-mouse immune cell surface markers for 45 min at 4°C (anti-CD45-PE-Cy5, anti-CD11b-APC-CY7, anti-CD4-e450, anti-CD8-AF700, anti-MHC class II-APC, and anti-PD-1-PE, anti-Ki67-APC, and anti-PD-L1-PE or FITC (eBiosciences, San Diego, CA). Analysis by flow cytometry was performed. Control isotype Abs were used for all fluorochrome combinations to assess nonspecific Ab binding. Live leukocytes were gated using forward scatter and side scatter parameters on a BD FACSCanto flow cytometer

(BD Biosciences, San Jose, CA). Data was analyzed using FlowJo software (FlowJo, Ashland, OR).

Real-time RT-PCR

RNA from purified microglia and astrocyte cell cultures, or from brain tissue was extracted using an RNeasy Mini Kit (Qiagen, Valencia, CA) or TRIzol reagent (Invitrogen, Carlsbad, CA), respectively. cDNA was synthesized with 0.5 to 1.0 μg of total RNA using Superscript III reverse transcriptase (Invitrogen) and oligo $d(T)_{12–18}$ primers (Sigma-Aldrich). PCR was performed with the SYBR Advantage qPCR master mix (ClonTech, Mountain View, CA). The PCR conditions for the M×3000P QPCR System (Stratagene, now Agilent Technologies, La Jolla, CA) were: 1 denaturation cycle at 95°C for 10 s; 40 amplification cycles of 95o for 10 s, 60o annealing for 10 s, and elongation at 72°C for 10 s; followed by 1 dissociation cycle. The relative product levels were quantified using the $2^{-\Delta\Delta Ct}$ method (Livak and Schmittgen 2001) and were normalized to the housekeeping gene hypoxanthine phosphoribosyl transferase (HPRT).

Enzyme-linked immunosorbent assay (ELISA)

Homogenized animal brains in DMEM media containing 1% FBS were centrifuged at 4°C for 15 min to harvest supernatants followed by measurement using a protein assay reagent (Bio-Rad, Hercules, CA) before being used for ELISA. In brief, 96-well ELISA plates pre-coated with anti-mouse MHC class II, GFAP, IFN-g, CXCL10 or MAP-2 antibodies (2 mg/ml) overnight at 4°C were blocked with 1% BSA in PBS for 1h at 37°C. After washing (PBS with Tween 20), brain supernatants and a series of dilution of MHC class II, GFAP, IFN-g, CXCL10 or MAP-2 (as standards) were added to the wells for 2h at 37°C. Then, anti-MHC class II, GFAP, IFN-g, CXCL10 or MAP-2 detection antibodies were added for 90 min at 37°C followed by addition of secondary antibodies conjugated with horseradish peroxidase (1:10,000) for 45 min at 37°C. A chromogen substrate K-Blue was added for color development which was terminated with 1M H_2SO_4. The plate was read at 450 nm and MHC class II, GFAP, IFN-γ, CXCL10, or MAP-2 concentrations were extrapolated from the standard concentration curves.

Immunohistochemistry

Brains were harvested from infected mice that were perfused with serial washes of phosphate-buffered saline (PBS), 2% sodium nitrate to remove contaminating blood cells, and 4% paraformaldehyde. Murine brains were subsequently submerged in 4% paraformaldehyde for 24 h and transferred to 25% sucrose solution for 2 d prior to sectioning. After blocking (1× PBS, 10% normal goat serum and 0.3% Triton X-100) for 1 h at room temperature, brain sections (25 μm) were incubated overnight at 4°C with the following primary antibodies: rat anti-mouse MHC class II (10μg/mL; eBioscience), rabbit anti-GFAP (1:1500; DAKO, Carpenteria, CA), rabbit anti-ionized calcium binding adaptor molecule (Iba)1 (2 μg/mL; Wako Chemicals, Richmond, VA), rat anti-mouse CD8 (10 μg/mL; eBioscience), rat anti-mouse CD4 (10 μg/mL; R&D Systems, Minneapolis, MN), rat anti-Foxp3 (eBioscience), and rabbit anti-mouse MAP-2 (2 μg/mL; EMD Millipore, Billerica, MA). Brain sections were washed three times with PBS. After washing, secondary antibody (rhodamine- or FITC-conjugate) was added for 1 h at RT followed by nuclear

labeling with Hoechst 33342 (1 μg/ml; Chemicon, Temecula, CA) and viewing under a fluorescent microscope.

Barnes Maze

The Barnes maze is a dry-land maze test for spatial learning and memory consisting of a circular platform with 40 holes along the perimeter (Med-Associated, St. Albans, Vermont). During testing, animals received reinforcement to escape from the open platform surface to a small, dark chamber located under one of the holes called the “target box”. Data were acquired over 4 d using four trials per day. Latency was defined as the time it took to locate the target box. For the probe test on d 5, the escape box was covered and the time spent in each quadrant was compared to time spent in the goal zone (90 sec test), which previously contained the escape box.

Statistical analysis

For comparison of means of pairs a two-tailed Student’s T-test for paired samples was applied. For comparison of means of multiple groups, analysis of variance (ANOVA) was performed followed by Bonferroni-test.

Results

Tregs accumulate within the brain following viral infection

Previous studies using our well-established MCMV infection model have demonstrated that both $CD4^+$ and $CD8^+$ T lymphocytes enter the brain to control viral infection (Cheeran et al. 2004; Cheeran et al. 2005). To determine whether regulatory T-cells are present within the infiltrating $CD4^+$ lymphocyte population, we infected Foxp3-GFP transgenic mice and examined single cell suspensions of brain tissue using flow cytometry. Brain-infiltrating $CD4^+$ T-cells were first gated on from the $CD45^+CD11b^{low}$ leukocyte population and subsequently analyzed for expression of GFP. Results generated from these studies showed that $Foxp3^+$ Treg cells were detectable within the brain during both acute (7 dpi) and chronic (30 dpi) phases of infection (Fig. 1A). Immunohistochemical staining for Foxp3 antigen at 7, 14, 24, 30, and 60 dpi confirmed the accumulation of Treg cells within the brain and demonstrated their presence in various regions: ventricles (choroid plexus), parenchyma, and meninges (Fig. 1B). Similar immunohistochemical staining using anti-Foxp3 Abs on brain tissue at 4 dpi showed very few $Foxp3^+$ cells at this early time point, indicating that brain infiltration by Tregs occurred between 4 and 7 dpi.

Tregs can be depleted from infected brains

Because we determined that Treg cells were present in the brain in response to viral infection, we went on to examine whether they could be depleted from this tissue using DTx treatment of infected Foxp3-DTR-GFP animals (i.e., *in-vivo* $Foxp3^+$ cell ablation). In these experiments, DTx was dissolved in saline and administered by ip injection to Foxp3-DTR-GFP mice at a dose of 0.5 μg on the day of infection (d 0). Infected animals were then given a reduced dose of DTx (0.1 μg) at 1 and 4 dpi. (Fig. 2A). When Treg levels were assessed using flow cytometry, a marked reduction was observed in brain tissue from DTx-treated vs. untreated animals during acute infection (7 dpi), 0.96 ± 0.08% vs. 5.06 ± 1.67%,

respectively (Fig. 2B). The difference in Treg numbers between treatment groups was most striking during acute infection, as DTx is cleared from the host and Treg numbers rebound during the chronic phase of infection, 14 and 30 dpi (Fig. 2B). Finally, given the well-recognized immunosuppressive effects of Treg cells, it is possible that establishment of viral brain infection was compromised due to more potent neuroimmune responses associated with Treg-ablation. However, when sections of brain tissue from animals with or without DTx treatment were examined for β-gal expression from the recombinant viral genome, no effect of DTx treatment on the ability to establish viral brain infection was observed at 4 dpi (Fig. 2C).

Elevated accumulation of T lymphocytes in the brain following Treg depletion

We next examined the effect of Treg ablation on brain infiltration and accumulation of T lymphocytes. In Treg-deficient, MCMV-infected mice, we observed increased numbers of $CD8^+$ and $CD4^+$ T-cells within the brain when compared to Treg-sufficient animals. While Treg ablation had no significant effect on lymphocyte numbers at 7 dpi, robust differences in both $CD8^+$ and $CD4^+$ T-cell numbers were observed within the brain at later time points, 14 and 30 dpi (Fig. 3A). These data were confirmed through immunohistochemical staining which showed markedly elevated numbers of $CD4^+$ T-cells in the ventricles and meninges, as well as elevated $CD8^+$ T-cell numbers within the parenchyma of Treg-depleted animals (Fig. 3B).

In the draining cervical lymph nodes, we found elevated levels of $CD4^+$ T-cell proliferation (as detected using flow cytometry for Ki67) within DTx-treated mice at 7 and 14 dpi (i.e., 66.7% versus 16.3%, and 49.3% versus 9.79% for $CD4^+$ T-cells at 7 and 14 dpi, with and without DTx, respectively). Similar data were obtained when $CD8^+$ T-cells within the lymph nodes were examined at 7 and 14 dpi (i.e., 38.9% versus 13.3%, and 35.8% versus 7.59% for $CD8^+$ T-cells at 7 and 14 dpi, with and without DTx, respectively). Interestingly, $CD8^+$ T-cell proliferation in the draining lymph nodes clearly waned by 30 dpi regardless of DTx treatment (3.13% versus 1.54%, with and without DTx, respectively); while some residual $CD4^+$ T-cell proliferation within the cervical lymph nodes of treated animals may remain at 30 dpi (14.8% versus 2.61% with and without DTx, respectively).

Increased and prolonged microglial cell reactivity with Treg depletion

Previous flow cytometry studies of isolated brain mononuclear cells (BMNCs), along with specific gating on the microglial cell population ($CD45^{int}CD11b^+$), showed that these cells upregulate the activation marker MHC class II during the acute phase of infection, and continue to chronically express this protein on their surface (Mutnal et al. 2011). More recently, we have demonstrated that brain-resident microglia also express PD-L1 (B7-H1) upon activation, which can suppress post-encephalitic $CD8^+$ lymphocytes (Schachtele et al. 2014).

We then went on to examine the expression kinetics of these surrogate markers of reactive microglia during viral brain infection in Treg-ablated vs. Treg-sufficient animals. While differences in MHC II expression during acute infection (7 dpi) were minor, Treg ablation resulted in increased and prolonged microglia cell reactivity over Treg-sufficient animals at

14 and 30 dpi (Fig. 4A). Similar elevated and prolonged microglial reactivity was observed when PD-L1 expression was used as an indicator, although its expression was higher during acute infection as well (Fig. 4B). In addition to cell percentage, DTx-treated animals also displayed significantly higher mean fluorescent intensity (MFI) for MHC II expression at 14 and 30 dpi, but differences in overall MFI were less apparent for PD-L1 expression and they did not reach statistical significance (Fig.4C and 4D, respectively).

The widespread and prolonged microglial cell reactivity following Treg depletion observed using flow cytometry was confirmed using immunohistochemistry. In post-encephalitic brains of MCMV-infected mice (40 dpi), Iba-1 was found to co-localize with MHC class II on reactive microglia. In both the meninges and parenchyma, greater staining was observed following DTx treatment (Fig. 5A). These data were quantified using ELISA for MHC class II expression in homogenates of brain tissues at 40 dpi. In these studies, significantly higher levels of MHC II protein was detected in homogenates from animals with Treg ablation compared to Treg-sufficient mice (Fig. 5B). Finally, morphological examination of Iba-1-stained microglia in infected brain tissues at 24 dpi demonstrated a more reactive phenotype associated with depletion of Treg cells, including formation of microglial nodules (Fig. 5C).

Tregs control microgliosis

Our next experiments investigated the effect of Tregs on microglial cell proliferation in response to viral brain infection. In the first study, BMNCs were isolated from infected animals; stained with anti-Ki67 antibody, which labels cells that are actively dividing; and examined by flow cytometry using the specific microglial cell gating strategy (i.e., $CD45^{int}CD11b^{+}$) described above. We found that while microglia from uninfected mice showed little proliferation, approximately half of the microglial cells isolated from infected brains were actively dividing during the acute phase of infection (7 dpi), (Fig. 6A). Interestingly, this proliferation quickly resolved and returned to baseline levels (Fig. 6A). To investigate the effect of Tregs, we compared microglial cell proliferation in infected Foxp3-DTR-GFP transgenic mice with or without DTx treatment. While marked differences between treatment groups were not observed during the acute phase of infection, increased and sustained reactive microgliosis was observed in Treg-depleted animals at the later time points tested (14 and 30 dpi) when compared to untreated, infected mice (Fig. 6B). The overall MFI for Ki67 expression in microglial cells was also elevated at 30 dpi (Fig. 6C).

Increased astrocyte reactivity with Treg depletion

We went on to investigate the effect of Treg ablation on astrocyte reactivity. Immunohistochemical staining of post-encephalitic brain (40 dpi) sections from Treg-depleted animals for GFAP displayed more astrocytes with a reactive phenotype in the cerebral cortex, ventricles, and hippocampus than corresponding sections from Treg-sufficient mice (Fig. 7A). The kinetics of GFAP mRNA expression were then examined using real-time RT-PCR. RNA isolated from brain homogenates collected from DTx-treated, Treg-ablated animals showed elevated and sustained expression of GFAP mRNA when compared to untreated, Treg-sufficient animals (Fig.7B). These data were confirmed and quantified at the protein level using ELISA, which showed significantly higher levels of

GFAP in brain homogenates obtained from animals with Treg ablation compared to Treg-sufficient mice at 40 dpi (Fig. 7C).

Tregs resolve post-encephalitic neuroinflammation

Having determined that Treg ablation promoted increased chronic reactive gliosis, we investigated whether it correspondingly prolonged the proinflammatory microenvironment within brain tissue following infection. In these studies, RNA was isolated from brain homogenates collected from untreated or DTx-treated, MCMV-infected animals and examined for expression of proinflammatory mediators by real-time RT-PCR. Results obtained showed elevated and sustained levels of mRNA expression for every mediator tested within the brains of Treg-depleted mice when compared to untreated, Treg-sufficient animals over the indicated time course (Fig.8A). These mRNA data were confirmed at the protein level through quantification of IFN-γ and CXCL10 using ELISA at 40 dpi (Fig.8B). Finally, expression of neuronal microtubule-associated protein (MAP)-2, as a surrogate marker of neurotoxicity, was found to be significantly diminished in the CA1 region of the hippocampus, as well as cerebral cortex, of animals which were treated for Treg ablation, quantified using ELISA (Fig. 8C).

Long-term neurological deficits with Treg depletion

Various means by which neuroimmune responses control viral brain infection have been elucidated, but studies of mechanisms underlying the long-term neurological sequelae observed following encephalitis have been more limited. We have previously found that T-cell brain-infiltration and chronic reactive gliosis following experimental herpes encephalitis in mice (Marques et al. 2008) was associated with deficits in spatial memory using the Morris water maze (Armien et al. 2010). The Barnes maze is a dry-land maze test, which also tests spatial learning and memory, in which animals receive reinforcement to escape from an open platform to a small, dark chamber located under one of the holes called the target box. Latency to escape is defined as the time it takes for an animal to locate the target box. Having detected neurotoxicity within the hippocampus, we next examined Foxp3-DTR-GFP mice with or without Treg ablation for deficiencies in spatial learning and memory using the Barnes maze. Groups of convalescent animals (n = 9–13/group) at 30 dpi were tested during 4 d of acquisition using four trials per day. Significant deficiencies in Treg-depleted mice were seen as early as d 3 of testing when compared to Treg-sufficient or uninfected animals (Fig. 9A). On test d 5, animals were assessed using a probe test in which the escape box was covered and the time spent in each quadrant was compared to time spent in the goal zone which previously contained the escape box. These results demonstrated that animals which received Treg depletion during acute infection were found to spend significantly less time in the goal zone than infected, undepleted or uninfected animals (Fig. 9B).

Discussion

Recent studies have demonstrated that $Foxp3^+$ Treg cells accumulate within brains of mice following infection with neurotropic viruses (Graham et al. 2014; Zhao et al. 2014). Results reported here show that accumulation and retention of these immunosuppressive cells within

the brain occurs concomitantly with chronic neuroinflammation observed following brain infection with MCMV (Mutnal et al. 2011). In addition, it has been reported that clinical disease during viral infection is more severe following depletion of the Treg population (Anghelina et al. 2009; Veiga-Parga et al. 2012). Because Tregs are well-known to negatively regulate the functions of effector T-cells, we extended these findings by showing that depletion of the Treg population from encephalitic brains not only leads to markedly elevated T-cell numbers, but prolongs chronic reactive phenotypes of the resident glial cells themselves.

While treatment of Foxp3-DTR-GFP mice with DTx (0–4 dpi) was found to clearly deplete Treg cells from the brain, the difference between treatment groups was most striking early during infection (7 dpi). The use of these transgenic animals is a standard approach for studying Treg effects *in vivo*, but it does produce a drastic, complete depletion of this important regulatory cell population, which may be a limitation of the model. Treg numbers within the brain quickly rebounded and were not markedly different by 14 dpi, which likely represents an effort by the immune system to re-establish proper homeostatic control. Paradoxically, it has previously been reported that the actual number of Treg cells is often elevated in target tissues during autoimmune and inflammatory diseases, but the inability of these tissue-infiltrating Tregs to modulate disease suggests that they may be functionally compromised, even though they are present in elevated numbers (Cao et al. 2003; Feger et al. 2007; Korn et al. 2007). Likewise, in this study, although numbers of Treg cells within the brain recovered by 14 dpi, the inability to suppress chronic glial cell reactivity suggests that the cells which replete the brains were functionally compromised. Similar findings have recently been reported using acute DTx depletion of Tregs in an experimental murine model of West Nile virus (WNV) encephalitis, where Treg numbers within the infected brain returned to steady state numbers by 20 dpi, yet development of long-term resident memory T-cell responses was impaired (Graham et al. 2014). While functional compromise of the Tregs which rebound following acute ablation is probable, it is also possible that the inflammatory milieu of the infected CNS may render effector T-cells and glial cells resistant to Treg-mediated suppression despite rebound of cell numbers. Another possible explanation may simply be a temporal delay between Treg effects and homing of infiltrating T-cells into the brain, which in turn may lead to more microgliosis and astrocytosis.

$CD8^+$ effector T-cells are essential for viral clearance following MCMV brain infection. So, it is possible that the loss of Treg-mediated negative regulation of anti-viral $CD8^+$ lymphocyte responses, occurring following Treg depletion, could affect the establishment of viral infection. However, our data show that MCMV infection was still established within the brains of animals receiving DTx treatment, when assessed at 4 dpi. A similar lack of impact of Treg depletion on viral distribution and clearance has been reported in MHV and WNV brain infection models (Cervantes-Barragan et al. 2012; Graham et al. 2014). Taken together, these findings suggest that the elevated long-term glial cell reactivity observed following Treg depletion was not simply due to altered viral infection.

Although Tregs are best known for their ability to limit immune responses to self-Ags and prevent autoimmunity, an increasing number of studies have demonstrated that viral infection promotes the development of pathogen-specific Treg cells (Bedoya et al. 2013;

Suffia et al. 2006; Zhao et al. 2011). Transfer of bulk Tregs along with effector T-cells has been reported to result in less severe clinical disease in MHV-infected $RAG^{-/-}$ animals (Trandem et al. 2010), but pathogen-specific Tregs were found to be even more potently-suppressive than bulk Tregs (Zhao et al. 2014). Since in our studies we did not examine Treg antigen specificity or determine the anatomical location of their development, in this manuscript we use the term Treg to refer to the $Foxp3^+$ $CD4^+$ T-cell population with suppressive activity, rather than using the more-specific terms tTreg or iTreg cells (Abbas et al. 2013). In humans, but not mice, Foxp3 has also been reported to be expressed in $CD4^+$ T-cells which were found to be hyporesponsive, but not necessarily suppressive (Morgan et al. 2005; Tran et al. 2007; Wang et al. 2007). These findings imply that there may be important differences between mice and humans regarding Foxp3 as a marker for Tregs.

Elevated, prolonged microglial cell reactivity and microgliosis were observed following Treg depletion. Two distinct populations of CD45+ mononuclear phagocytes ($CD45^{hi}$ and $CD45^{int}$) can be detected within virus-infected brains (Sedgwick et al. 1991). During MCMV infection, we have previously demonstrated that the brain-infiltrating $CD45^{hi}$ macrophage population is present within the CNS at early times (3 d), but not late times (30 d) post-infection (Mutnal et al. 2011). It has recently been shown that removal of Treg cells is associated with a reduction in alternatively activated macrophages at the site of traumatic injury (Walsh et al. 2014). However, in our MCMV brain infection model, brain-infiltrating macrophages are completely absent by 30 dpi. Resident microglial cells (i.e., the $CD45^{int}$ population) are derived from yolk sac progenitors which seed the brain early during development and represent a cell population which is genetically distinct from bone marrow-derived macrophages (i.e., $CD45^{hi}$) (Ginhoux et al. 2010; Kierdorf et al. 2013). It is only these $CD45^{int}$ cells which can be detected within the brains of sham-, mock- or uninfected animals. In this study, we specifically gated on the $CD45^{int}CD11b^{hi}$ microglial cell population to assess various markers of cellular activation.

Our previous publications have reported that resting microglia (i.e., $CD45^{int}CD11b^{hi}$ cells) from uninfected murine brains express very low constitutive levels of MHC class II (<5%). However, following herpesvirus brain infection (using either HSV-1 or MCMV), MHC class II expression is strikingly upregulated on >90% of these cells (Marques et al. 2008; Mutnal et al. 2011). These data demonstrate the utility of MHC II expression as a surrogate marker of microglial cell reactivity in response to proinflammatory conditions. Likewise, a low basal level of PD-L1 expression is also observed on approximately 20% of microglia from uninfected mice, but induced expression is detectable on over 90% of the cells within one week following infection (Magnus et al. 2005; Schachtele et al. 2014). Like MHC II, these data demonstrate the utility of PD-L1 expression as a surrogate activation marker. Here, Treg cell ablation increased the level of prolonged microglial cell reactivity, in response to infection, as determined through expression of both of these surrogate activation markers. In addition, Iba-1-staining of microglia in infected brain tissues demonstrated a greater number of cells with a reactive phenotype following depletion of Tregs. Interestingly, data presented in Fig. 6 show that brain-resident microglial cells proliferated during the acute phase of viral infection (7 dpi). While this proliferation quickly returns to baseline in Treg sufficient animals, sustained reactive microgliosis was observed in Treg-depleted mice.

Astrocytes were the first glial cells on which MHC II was shown to be inducible (Lipp et al. 2007; Shrikant and Benveniste 1996). In comparison to microglia, expression on astrocytes is slower to develop and less robust, thus deeming them “non-professional” antigen presenting cells (Vardjan et al. 2012). While few studies have addressed interactions between Tregs and astrocytes, *in vitro* experiments have shown that murine primary astrocytes polarize $CD4^+$ T-cells into Tregs, as well as Th1 subtypes (Beurel et al. 2014). Like microglia, astrocytes also acquire reactive phenotypes in response to proinflammatory environments. This phenotype is routinely visualized through immunostaining for GFAP, and quantified by assessing its expression level. Here, we assessed GFAP mRNA expression levels using real-time RT-PCR, as well as its protein level using ELISA, and found it to be significantly higher in animals with Treg ablation compared to Treg sufficient mice. Data presented here indicate that brain-infiltrating Treg cells also exert suppressive effects on astrocyte reactivity, astrogliosis, and subsequent glial scaring.

A shift from the normal anti-inflammatory brain microenvironment to a more pro-inflammatory state occurs in many diseases of the CNS. We have previously shown that our MCMV brain infection model results in chronic neuroinflammation that persists following viral clearance, and in the absence of detectable viral antigen (Mutnal et al. 2011). We went on to show that IFN-γ secretion by brain-infiltrating T-cells is responsible for long-term microglial activation and tumor necrosis factor (TNF)-α production (Mutnal et al. 2011). IFN-γ has also been shown to induce microglia expression of T-cell co-stimulatory molecules (CD80 & CD86) that are necessary second-signals for glia to functionally activate T-cells (Aloisi 2001). In addition, synergistic action between TNF-α and IFN-γ in the brain has been shown to increase nitric oxide-induced neurodegeneration (Blais and Rivest 2004), emphasizing the importance of minimizing chronic neuroinflammation. Tregs are well known to modulate microglial cell-produced reactive oxygen species and, correspondingly, suppress microglia-induced neurotoxicity (Reynolds et al. 2009; Zhao et al. 2012).Here, the increased proinflammatory brain microenvironment observed following depletion of Tregs during acute viral infection was associated with heightened neuronal damage when MAP-2 expression was assessed, as a surrogate marker of neurotoxicity. Although the exact mechanisms by which Tregs down-regulate inflammation remain to be elucidated, these cells are well-known to produce high levels of IL-10 (McGeachy and Anderton 2005; Rubtsov et al. 2008), which is well-known to regulate neuroinflammation. If not carefully managed, this extended inflammation of the brain can lead to secondary neuronal injury and resultant neurocognitive dysfunction.

Overactive, persistent immune activation can be detrimental to sensitive neuronal cells resulting in focal neuropathology and, correspondingly, behavioral deficits (Armien et al. 2010). Reactive microglial cells have been linked to synaptic dysfunction and loss, which has been shown to affect learning and memory, reviewed in (Morris et al. 2013). Picornavirus-induced memory deficits have been correlated to the level of hippocampal damage following experimental encephalitis (Buenz et al. 2006). Additionally, the immunoregulatory properties of Treg cells which recognize CNS antigens have also been linked to neurogenesis, learning, and memory in immunodeficient animals (Kipnis et al. 2004; Ziv et al. 2006). Here, we report that MCMV infection-induced, long-term neurological deficits in spatial learning and memory following Treg depletion are associated

with chronic reactive gliosis. Taken together, impaired neural, cognitive, and behavioral functioning is commonly seen in patients recovering from infection-induced neuroinflammation. We anticipate that studies using murine models, like those presented here, will provide critical insights into the central role of Tregs in modulating these disorders.

Acknowledgements

This project was supported by grants from the National Institute of Mental Health (MH-066703) and the National Institute of Neurological Disorders and Stroke (NS-038836). The funders had no role in study design, data collection and analysis, decision to publish, or preparation of the manuscript. We thank Racheal Fischer and the NINDS University of Minnesota Behavioral Phenotyping Core for behavioral analysis.

References

Abbas AK, Benoist C, Bluestone JA, Campbell DJ, Ghosh S, Hori S, Jiang S, Kuchroo VK, Mathis D, Roncarolo MG, et al. Regulatory T cells: recommendations to simplify the nomenclature. Nat Immunol. 2013; 14(4):307–308. [PubMed: 23507634]

Aloisi F. Immune function of microglia. Glia. 2001; 36(2):165–179. [PubMed: 11596125]

Anghelina D, Zhao J, Trandem K, Perlman S. Role of regulatory T cells in coronavirus-induced acute encephalitis. Virology. 2009; 385(2):358–367. [PubMed: 19141357]

Armien AG, Hu S, Little MR, Robinson N, Lokensgard JR, Low WC, Cheeran MC. Chronic cortical and subcortical pathology with associated neurological deficits ensuing experimental herpes encephalitis. Brain Pathol. 2010; 20(4):738–750. [PubMed: 20002440]

Bedoya F, Cheng GS, Leibow A, Zakhary N, Weissler K, Garcia V, Aitken M, Kropf E, Garlick DS, Wherry EJ, et al. Viral antigen induces differentiation of Foxp3+ natural regulatory T cells in influenza virus-infected mice. J Immunol. 2013; 190(12):6115–6125. [PubMed: 23667113]

Beurel E, Harrington LE, Buchser W, Lemmon V, Jope RS. Astrocytes modulate the polarization of CD4+ T cells to Th1 cells. PLoS One. 2014; 9(1):e86257. [PubMed: 24489707]

Blais V, Rivest S. Effects of TNF-alpha and IFN-gamma on nitric oxide-induced neurotoxicity in the mouse brain. J Immunol. 2004; 172(11):7043–7052. [PubMed: 15153526]

Buenz EJ, Rodriguez M, Howe CL. Disrupted spatial memory is a consequence of picornavirus infection. Neurobiol Dis. 2006; 24(2):266–273. [PubMed: 16919964]

Burda JE, Sofroniew MV. Reactive gliosis and the multicellular response to CNS damage and disease. Neuron. 2014; 81(2):229–248. [PubMed: 24462092]

Cao D, Malmstrom V, Baecher-Allan C, Hafler D, Klareskog L, Trollmo C. Isolation and functional characterization of regulatory CD25brightCD4+ T cells from the target organ of patients with rheumatoid arthritis. Eur J Immunol. 2003; 33(1):215–223. [PubMed: 12594850]

Cervantes-Barragan L, Firner S, Bechmann I, Waisman A, Lahl K, Sparwasser T, Thiel V, Ludewig B. Regulatory T cells selectively preserve immune privilege of self-antigens during viral central nervous system infection. J Immunol. 2012; 188(8):3678–3685. [PubMed: 22407917]

Cheeran MC, Gekker G, Hu S, Min X, Cox D, Lokensgard JR. Intracerebral infection with murine cytomegalovirus induces CXCL10 and is restricted by adoptive transfer of splenocytes. J Neurovirol. 2004; 10(3):152–162. [PubMed: 15204920]

Cheeran MC, Gekker G, Hu S, Palmquist JM, Lokensgard JR. T cell-mediated restriction of intracerebral murine cytomegalovirus infection displays dependence upon perforin but not interferon-gamma. J Neurovirol. 2005; 11(3):274–280. [PubMed: 16036807]

Cheeran MC, Hu S, Palmquist JM, Bakken T, Gekker G, Lokensgard JR. Dysregulated interferon-gamma responses during lethal cytomegalovirus brain infection of IL-10-deficient mice. Virus Res. 2007; 130(1–2):96–102. [PubMed: 17624463]

Ertelt JM, Rowe JH, Mysz MA, Singh C, Roychowdhury M, Aguilera MN, Way SS. Foxp3+ regulatory T cells impede the priming of protective CD8+ T cells. J Immunol. 2011; 187(5):2569–2577. [PubMed: 21810602]

Feger U, Luther C, Poeschel S, Melms A, Tolosa E, Wiendl H. Increased frequency of CD4+ CD25+ regulatory T cells in the cerebrospinal fluid but not in the blood of multiple sclerosis patients. Clin Exp Immunol. 2007; 147(3):412–418. [PubMed: 17302889]

Fontenot JD, Rasmussen JP, Williams LM, Dooley JL, Farr AG, Rudensky AY. Regulatory T cell lineage specification by the forkhead transcription factor foxp3. Immunity. 2005; 22(3):329–341. [PubMed: 15780990]

Ford AL, Goodsall AL, Hickey WF, Sedgwick JD. Normal adult ramified microglia separated from other central nervous system macrophages by flow cytometric sorting. Phenotypic differences defined and direct ex vivo antigen presentation to myelin basic protein-reactive CD4+ T cells compared. J Immunol. 1995; 154(9):4309–4321. [PubMed: 7722289]

Ginhoux F, Greter M, Leboeuf M, Nandi S, See P, Gokhan S, Mehler MF, Conway SJ, Ng LG, Stanley ER, et al. Fate mapping analysis reveals that adult microglia derive from primitive macrophages. Science. 2010; 330(6005):841–845. [PubMed: 20966214]

Graham JB, Da Costa A, Lund JM. Regulatory T cells shape the resident memory T cell response to virus infection in the tissues. J Immunol. 2014; 192(2):683–690. [PubMed: 24337378]

Kierdorf K, Erny D, Goldmann T, Sander V, Schulz C, Perdiguero EG, Wieghofer P, Heinrich A, Riemke P, Holscher C, et al. Microglia emerge from erythromyeloid precursors via Pu.1- and Irf8-dependent pathways. Nat Neurosci. 2013; 16(3):273–280. [PubMed: 23334579]

Kim JM, Rasmussen JP, Rudensky AY. Regulatory T cells prevent catastrophic autoimmunity throughout the lifespan of mice. Nat Immunol. 2007; 8(2):191–197. [PubMed: 17136045]

Kipnis J, Cohen H, Cardon M, Ziv Y, Schwartz M. T cell deficiency leads to cognitive dysfunction: implications for therapeutic vaccination for schizophrenia and other psychiatric conditions. Proc Natl Acad Sci U S A. 2004; 101(21):8180–8185. [PubMed: 15141078]

Korn T, Reddy J, Gao W, Bettelli E, Awasthi A, Petersen TR, Backstrom BT, Sobel RA, Wucherpfennig KW, Strom TB, et al. Myelin-specific regulatory T cells accumulate in the CNS but fail to control autoimmune inflammation. Nat Med. 2007; 13(4):423–431. [PubMed: 17384649]

Lanteri MC, O'Brien KM, Purtha WE, Cameron MJ, Lund JM, Owen RE, Heitman JW, Custer B, Hirschkorn DF, Tobler LH, et al. Tregs control the development of symptomatic West Nile virus infection in humans and mice. J Clin Invest. 2009; 119(11):3266–3277. [PubMed: 19855131]

Lipp M, Brandt C, Dehghani F, Kwidzinski E, Bechmann I. PD-L1 (B7-H1) regulation in zones of axonal degeneration. Neurosci Lett. 2007; 425(3):156–161. [PubMed: 17825988]

Livak KJ, Schmittgen TD. Analysis of relative gene expression data using real-time quantitative PCR and the 2(-Delta Delta C(T)) Method. Methods. 2001; 25(4):402–408. [PubMed: 11846609]

Magnus T, Schreiner B, Korn T, Jack C, Guo H, Antel J, Ifergan I, Chen L, Bischof F, Bar-Or A, et al. Microglial expression of the B7 family member B7 homolog 1 confers strong immune inhibition: implications for immune responses and autoimmunity in the CNS. J Neurosci. 2005; 25(10):2537–2546. [PubMed: 15758163]

Marques CP, Cheeran MC, Palmquist JM, Hu S, Urban SL, Lokensgard JR. Prolonged microglial cell activation and lymphocyte infiltration following experimental herpes encephalitis. J Immunol. 2008; 181(9):6417–6426. [PubMed: 18941232]

Marten NW, Stohlman SA, Zhou J, Bergmann CC. Kinetics of virus-specific CD8+ -T-cell expansion and trafficking following central nervous system infection. J Virol. 2003; 77(4):2775–2778. [PubMed: 12552021]

McGeachy MJ, Anderton SM. Cytokines in the induction and resolution of experimental autoimmune encephalomyelitis. Cytokine. 2005; 32(2):81–84. [PubMed: 16153854]

McPherson SW, Heuss ND, Roehrich H, Gregerson DS. Bystander killing of neurons by cytotoxic T cells specific for a glial antigen. Glia. 2006; 53(5):457–466. [PubMed: 16355370]

Morgan ME, van Bilsen JH, Bakker AM, Heemskerk B, Schilham MW, Hartgers FC, Elferink BG, van der Zanden L, de Vries RR, Huizinga TW, et al. Expression of FOXP3 mRNA is not confined to CD4+CD25+ T regulatory cells in humans. Hum Immunol. 2005; 66(1):13–20. [PubMed: 15620457]

Morris GP, Clark IA, Zinn R, Vissel B. Microglia: a new frontier for synaptic plasticity, learning and memory, and neurodegenerative disease research. Neurobiol Learn Mem. 2013; 105:40–53. [PubMed: 23850597]

Mutnal MB, Hu S, Little MR, Lokensgard JR. Memory T cells persisting in the brain following MCMV infection induce long-term microglial activation via interferon-gamma. J Neurovirol. 2011; 17(5):424–437. [PubMed: 21800103]

Mutnal MB, Hu S, Lokensgard JR. Persistent humoral immune responses in the CNS limit recovery of reactivated murine cytomegalovirus. PLoS One. 2012; 7(3):e33143. [PubMed: 22412996]

Mutnal MB, Hu S, Schachtele SJ, Lokensgard JR. Infiltrating regulatory B cells control neuroinflammation following viral brain infection. J Immunol. 2014; 193(12):6070–6080. [PubMed: 25385825]

Neumann H. Control of glial immune function by neurons. Glia. 2001; 36(2):191–199. [PubMed: 11596127]

Reddehase MJ, Mutter W, Munch K, Buhring HJ, Koszinowski UH. CD8-positive T lymphocytes specific for murine cytomegalovirus immediate-early antigens mediate protective immunity. J Virol. 1987; 61(10):3102–3108. [PubMed: 3041033]

Reynolds AD, Stone DK, Mosley RL, Gendelman HE. Nitrated {alpha}-synuclein-induced alterations in microglial immunity are regulated by CD4+ T cell subsets. J Immunol. 2009; 182(7):4137–4149. [PubMed: 19299711]

Rubtsov YP, Rasmussen JP, Chi EY, Fontenot J, Castelli L, Ye X, Treuting P, Siewe L, Roers A, Henderson WR Jr, et al. Regulatory T cell-derived interleukin-10 limits inflammation at environmental interfaces. Immunity. 2008; 28(4):546–558. [PubMed: 18387831]

Schachtele SJ, Hu S, Sheng WS, Mutnal MB, Lokensgard JR. Glial cells suppress postencephalitic CD8+ T lymphocytes through PD-L1. Glia. 2014; 62(10):1582–1594. [PubMed: 24890099]

Sedgwick JD, Schwender S, Imrich H, Dorries R, Butcher GW, ter Meulen V. Isolation and direct characterization of resident microglial cells from the normal and inflamed central nervous system. Proc Natl Acad Sci U S A. 1991; 88(16):7438–7442. [PubMed: 1651506]

Shrikant P, Benveniste EN. The central nervous system as an immunocompetent organ: role of glial cells in antigen presentation. J Immunol. 1996; 157(5):1819–1822. [PubMed: 8757296]

Stoddart CA, Cardin RD, Boname JM, Manning WC, Abenes GB, Mocarski ES. Peripheral blood mononuclear phagocytes mediate dissemination of murine cytomegalovirus. J Virol. 1994; 68(10):6243–6253. [PubMed: 8083964]

Suffia IJ, Reckling SK, Piccirillo CA, Goldszmid RS, Belkaid Y. Infected site-restricted Foxp3+ natural regulatory T cells are specific for microbial antigens. J Exp Med. 2006; 203(3):777–788. [PubMed: 16533885]

Suvas S, Azkur AK, Kim BS, Kumaraguru U, Rouse BT. CD4+CD25+ regulatory T cells control the severity of viral immunoinflammatory lesions. J Immunol. 2004; 172(7):4123–4132. [PubMed: 15034024]

Tran DQ, Ramsey H, Shevach EM. Induction of FOXP3 expression in naive human CD4+FOXP3 T cells by T-cell receptor stimulation is transforming growth factor-beta dependent but does not confer a regulatory phenotype. Blood. 2007; 110(8):2983–2990. [PubMed: 17644734]

Trandem K, Anghelina D, Zhao J, Perlman S. Regulatory T cells inhibit T cell proliferation and decrease demyelination in mice chronically infected with a coronavirus. J Immunol. 2010; 184(8):4391–4400. [PubMed: 20208000]

Vardjan N, Gabrijel M, Potokar M, Svajger U, Kreft M, Jeras M, de Pablo Y, Faiz M, Pekny M, Zorec R. IFN-gamma-induced increase in the mobility of MHC class II compartments in astrocytes depends on intermediate filaments. J Neuroinflammation. 2012; 9:144. [PubMed: 22734718]

Veiga-Parga T, Sehrawat S, Rouse BT. Role of regulatory T cells during virus infection. Immunol Rev. 2013; 255(1):182–196. [PubMed: 23947355]

Veiga-Parga T, Suryawanshi A, Mulik S, Gimenez F, Sharma S, Sparwasser T, Rouse BT. On the role of regulatory T cells during viral-induced inflammatory lesions. J Immunol. 2012; 189(12):5924–5933. [PubMed: 23129753]

Walsh JT, Zheng J, Smirnov I, Lorenz U, Tung K, Kipnis J. Regulatory T cells in central nervous system injury: a double-edged sword. J Immunol. 2014; 193(10):5013–5022. [PubMed: 25320276]

Wang J, Ioan-Facsinay A, van der Voort EI, Huizinga TW, Toes RE. Transient expression of FOXP3 in human activated nonregulatory CD4+ T cells. Eur J Immunol. 2007; 37(1):129–138. [PubMed: 17154262]

Zhao J, Zhao J, Fett C, Trandem K, Fleming E, Perlman S. IFN-gamma- and IL-10-expressing virus epitope-specific Foxp3(+) T reg cells in the central nervous system during encephalomyelitis. J Exp Med. 2011; 208(8):1571–1577. [PubMed: 21746812]

Zhao J, Zhao J, Perlman S. Virus-specific regulatory T cells ameliorate encephalitis by repressing effector T cell functions from priming to effector stages. PLoS Pathog. 2014; 10(8):e1004279. [PubMed: 25102154]

Zhao W, Beers DR, Liao B, Henkel JS, Appel SH. Regulatory T lymphocytes from ALS mice suppress microglia and effector T lymphocytes through different cytokine-mediated mechanisms. Neurobiol Dis. 2012; 48(3):418–428. [PubMed: 22820142]

Ziv Y, Ron N, Butovsky O, Landa G, Sudai E, Greenberg N, Cohen H, Kipnis J, Schwartz M. Immune cells contribute to the maintenance of neurogenesis and spatial learning abilities in adulthood. Nat Neurosci. 2006; 9(2):268–275. [PubMed: 16415867]

Main Points

- Elevated levels of encephalitic T lymphocytes are present following regulatory T-cell depletion during acute viral brain infection.
- Chronic microglial cell and astrocyte reactivity are observed subsequent to regulatory T-cell ablation.
- Unremitting neuroinflammation following regulatory T-cell depletion is associated with reduced cognitive performance by convalescent animals.

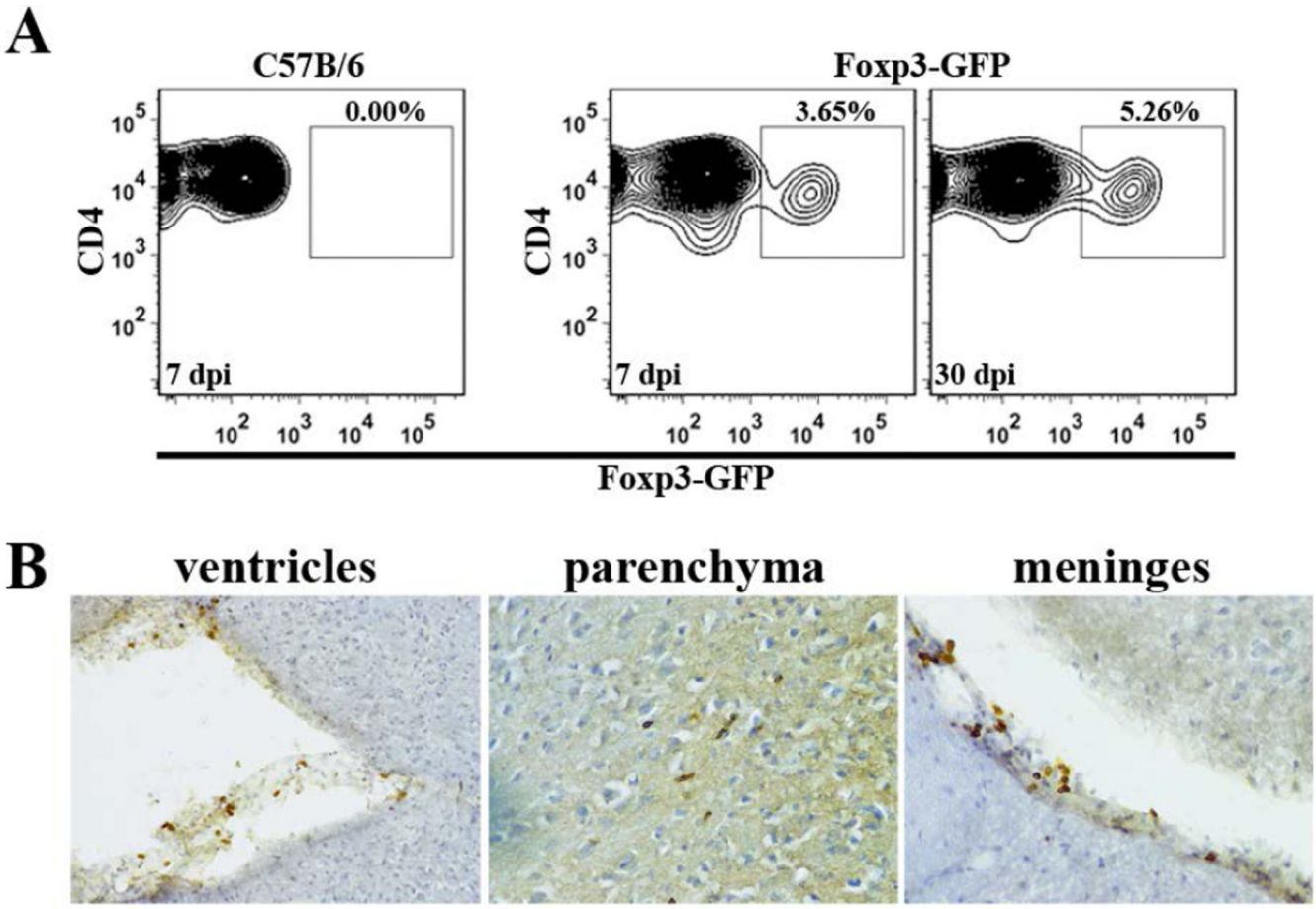

Figure 1. Tregs accumulate in post-encephalitic brains following viral infection

(A) Brain tissue from MCMV-infected, Foxp3-GFP transgenic mice was collected at 7 and 30 dpi. Brain-infiltrating leukocytes were isolated and stained for flow cytometry. $CD4^+$ T-cells were gated on from the $CD45^+CD11b^{low}$ leukocyte population for analysis of Foxp3-GFP expression. Infected wild-type C57B/6 animals (7 dpi) were included as a gating control. Contour plots shown are representative of two separate experiments using three animals/time point. **(B)** Flow cytometry data were confirmed using immunohistochemical staining for Foxp3, which demonstrated presence of T regulatory cells in the ventricles, parenchyma, and meninges of infected mice at 24 dpi.

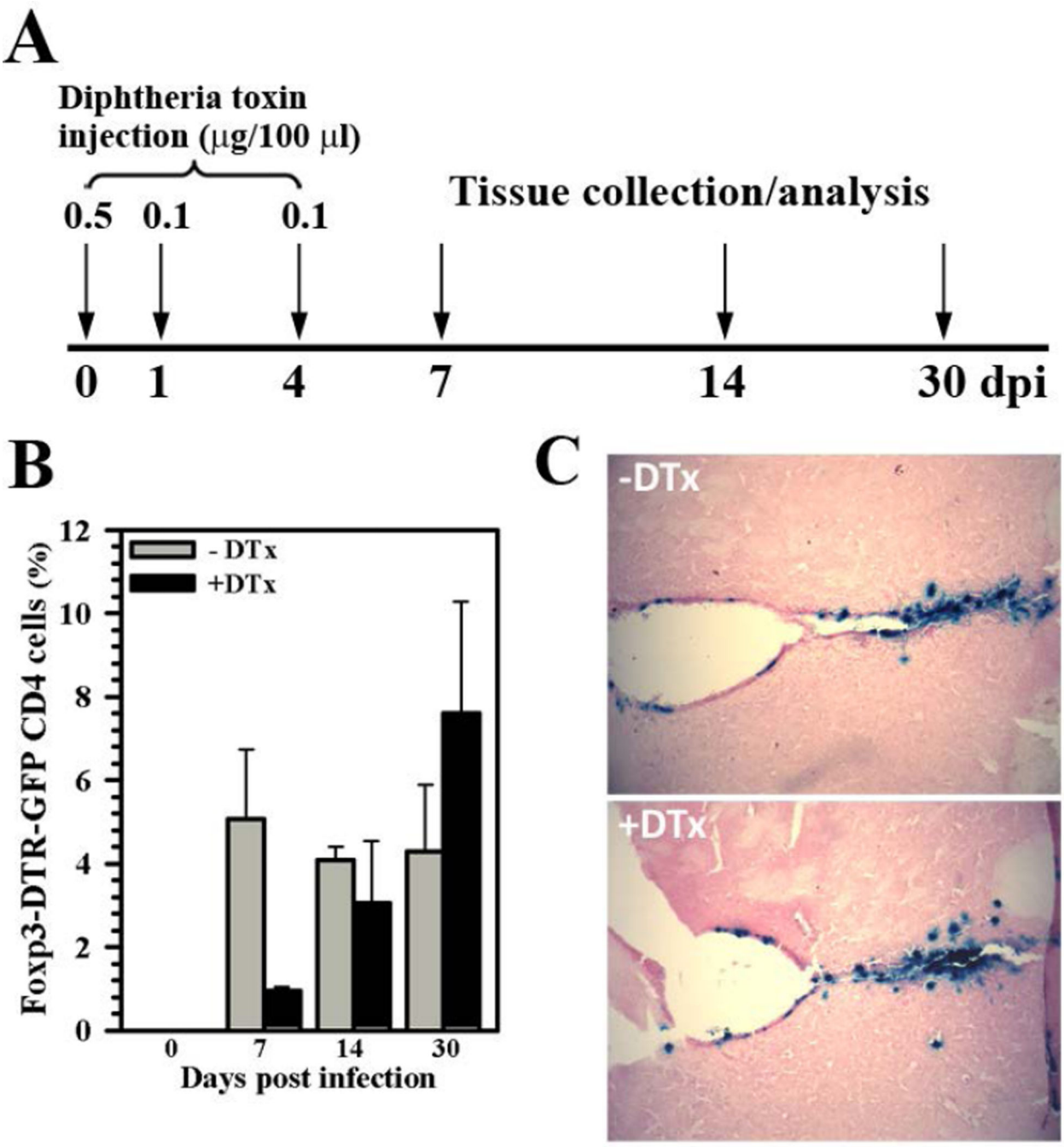

Figure 2. DTx treatment depletes Tregs from the brain but still allows establishment of viral infection

(A) Foxp3-DTR-GFP transgenic mice were injected with diphtheria toxin (DTx) at 0 (0.5 μg), 1 (0.1 μg), and 4 (0.1 μg) dpi to deplete Treg cells during the acute phase of viral brain infection. **(B)** To quantify Treg depletion from the brain, leukocytes were isolated from untreated (−DTx) as well as DTx-treated (+DTx), MCMV-infected mice and stained for flow cytometry to detect Foxp3-GFP expression within the $CD4^+$ subpopulation of brain-infiltrating T lymphocytes ($CD45^+CD11b^{low}$). Pooled data are presented as mean ± SEM of

two separate experiments using six animals per treatment group/time point. **(C)** Establishment of viral brain infection with or without DTx treatment was confirmed using X-gal (blue) staining to detect β-gal expression from the recombinant MCMV viral genome at 4 dpi.

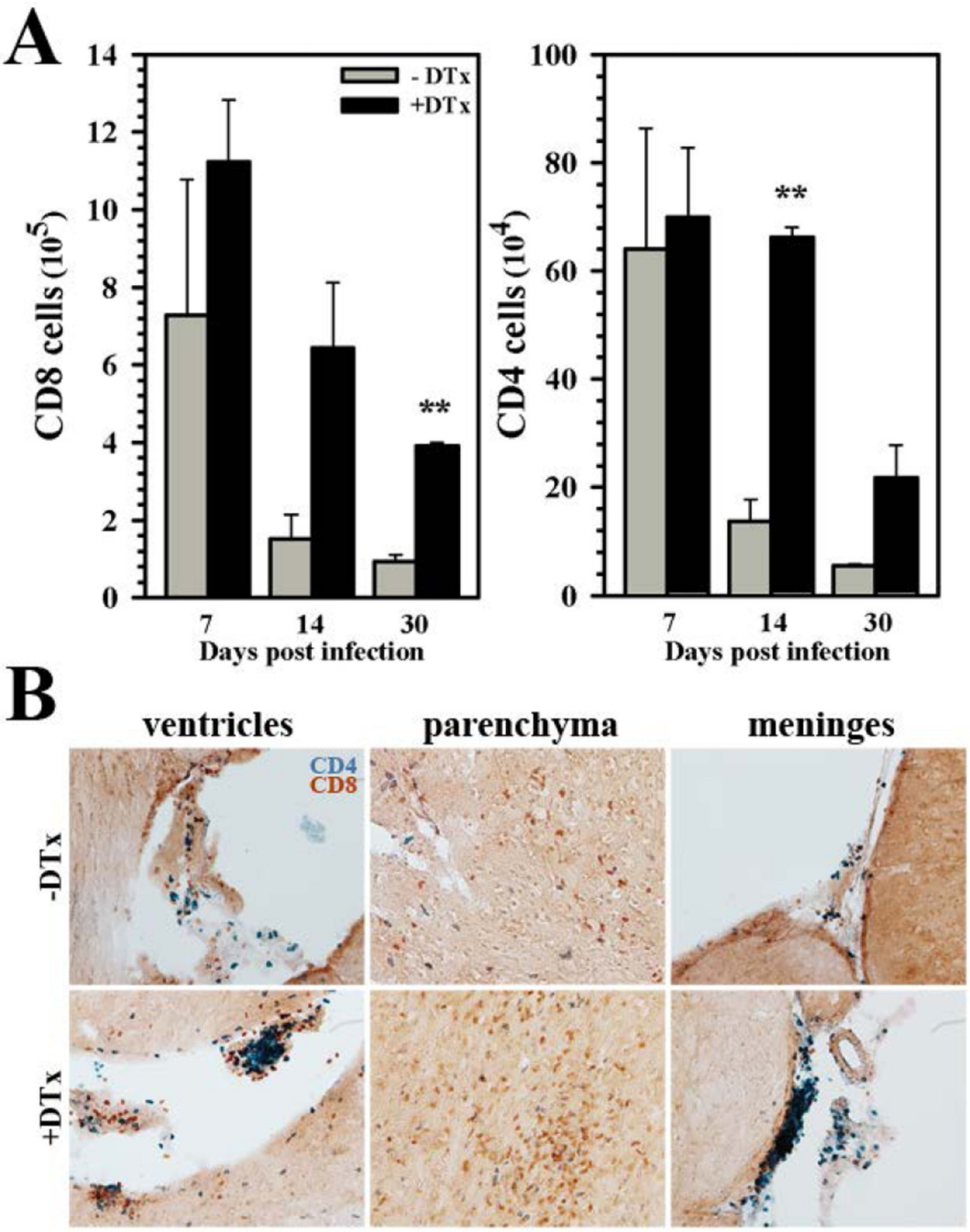

Figure 3. Elevated levels of encephalitic T-cells within infected brains of animals following acute Treg depletion

(A) Absolute numbers of $CD8^+$ and $CD4^+$ T-cells were calculated based on flow cytometric analysis of these populations isolated from the brains of MCMV-infected mice with or without DTx treatment during the acute phase of infection (as described in Figure 2). Lymphocyte numbers within the brain were determined at 7, 14, and 30 dpi. Pooled data are presented as mean ± SEM of two experiments using six animals per treatment group/time point. **(B)** Immunohistochemical staining for $CD4^+$ (blue) and $CD8^+$ (red) T lymphocytes

within the ventricles, parenchyma, and meninges of infected animals at 24 dpi with (+DTx) or without (−DTx) DTx treatment. **P ≤ 0.01 vs. −DTx.

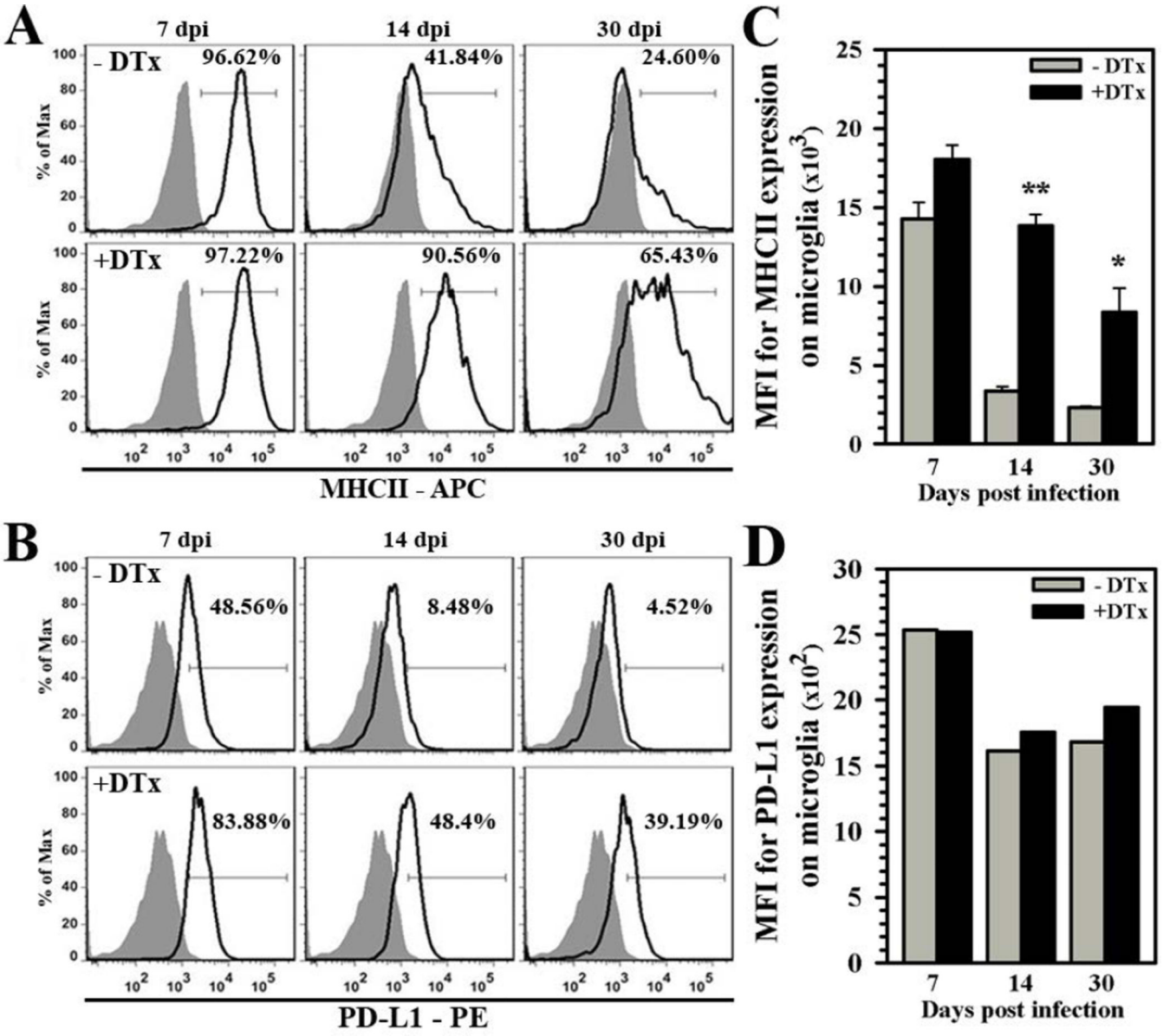

Figure 4. Elevated chronic microglial cell reactivity following Treg depletion during acute infection

Mononuclear cells were extracted from brains of untreated and DTx-treated mice infected with MCMV (7, 14, and 30 dpi). Microglia were first identified as $CD45^{int}CD11b^{+}$ cells and subsequently stained for surface indicators of reactive cells using antibodies against **(A)** MHC class II (APC-conjugated) and **(B)** PD-L1 (PE-conjugated). Isotype antibody control = filled grey line. Flow plots are representative of two separate experiments using three animals per group/experiment. **(C)** Data presented show MFI of MHC II binding and **(D)** PD-L1 binding from treated (+DTx) and untreated (−DTx) infected animals at the indicated time points. **P ≤ 0.01 vs. −DTx. *P ≤ 0.05 vs. −DTx.

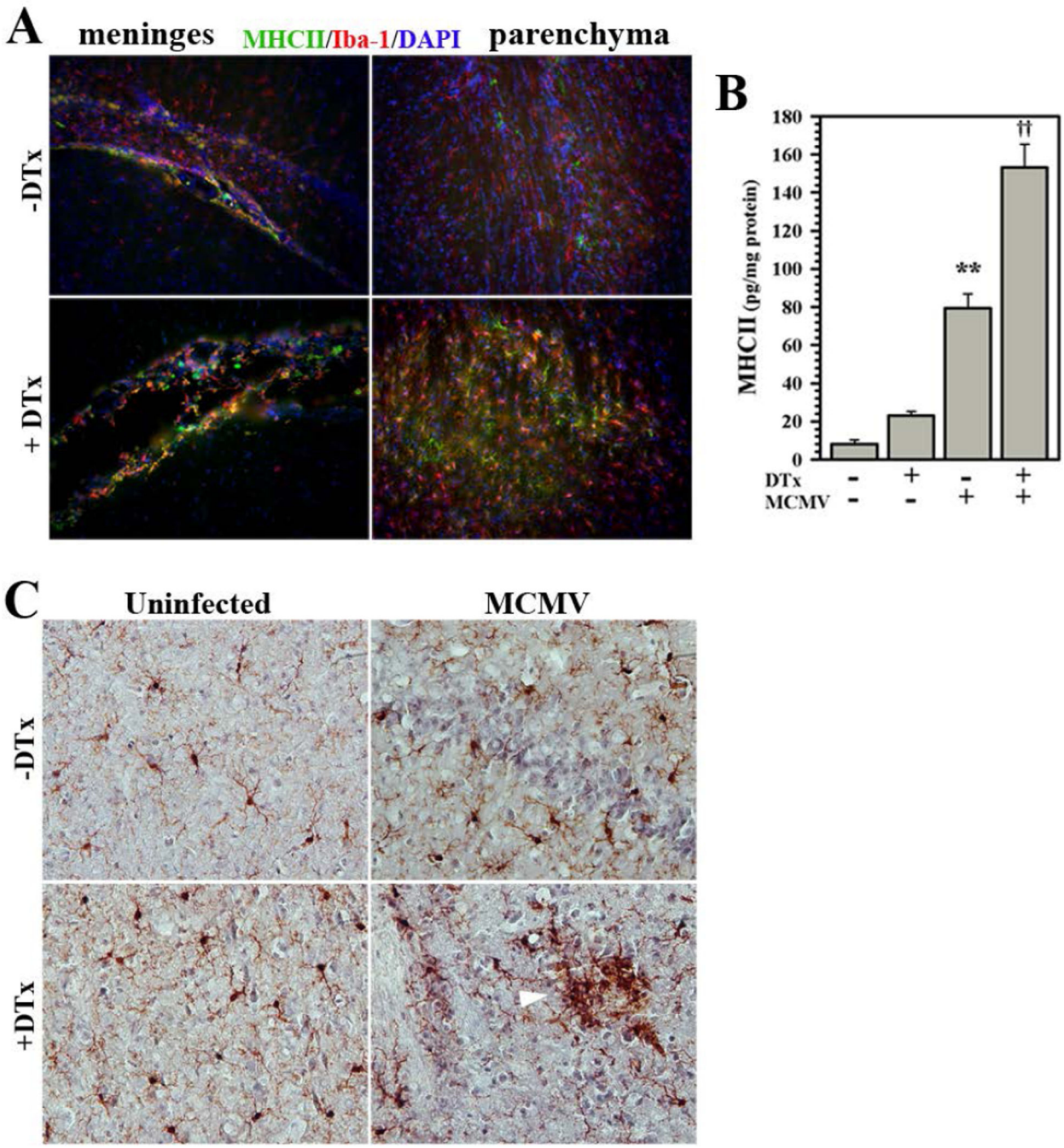

Figure 5. Immunohistochemical staining of chronic reactive microglia

Microglia chronically express MHC Class II and PD-L1 following MCMV brain infection. **(A)** Infected Foxp3-DTR-GFP transgenic mice with (+DTx) and without (−DTx) DTx treatment were perfused and brains were cryosectioned for immunohistochemistry. Co-labeling of MHC II (green), as an indicator of cell reactivity, and the microglial cell marker Iba-1 (red) was observed in the meninges and brain parenchyma at 40 dpi. **(B)** Elevated MHC Class II protein levels in chronically-infected brains with or without Treg depletion (±DTx) were quantified using ELISA. Pooled data presented are derived from three to nine

animals/group at 40 dpi. **(C)** Brain sections from infected animals ±DTx treatment stained for Iba-1 at 24 dpi displayed microglial nodules with reactive morphology (white arrow). **P ≤ 0.01 vs. uninfected. ††P ≤ 0.01 vs. MCMV.

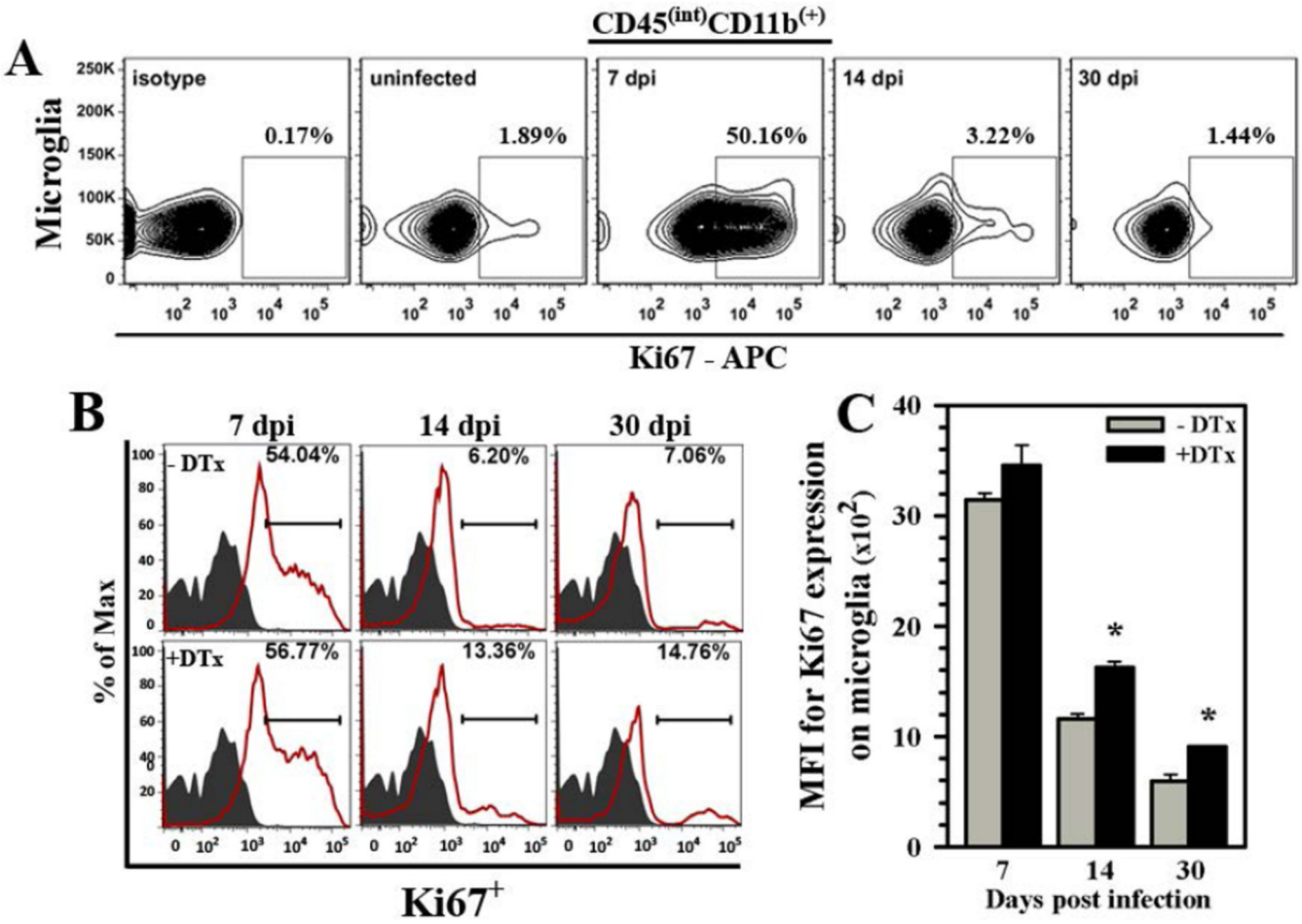

Figure 6. Treg cells control microgliosis during viral brain infection

(A) Flow cytometry was used to analyze microglia (i.e., $C45^{int}CD11b^{+}$) from Foxp3-GFP animals for active cell division in response to infection using anti-Ki67 (APC-conjugated), which labels dividing cells. Representative contour plot shows the kinetics of microgliosis. **(B)** Microgliosis during brain infection of Foxp3-DTR-GFP transgenic mice was compared in the presence (−DTx) and absence (+DTx) of regulatory T-cells (red line and indicated percentage). Isotype antibody control = filled grey line. Histograms presented are representative of two separate experiments using three infected animals per group/experiment. **(C)** Data presented show MFI for Ki67 expression from treated (+DTx) and untreated (−DTx) infected animals at the indicated time points post-infection. *P ≤ 0.05 vs. untreated

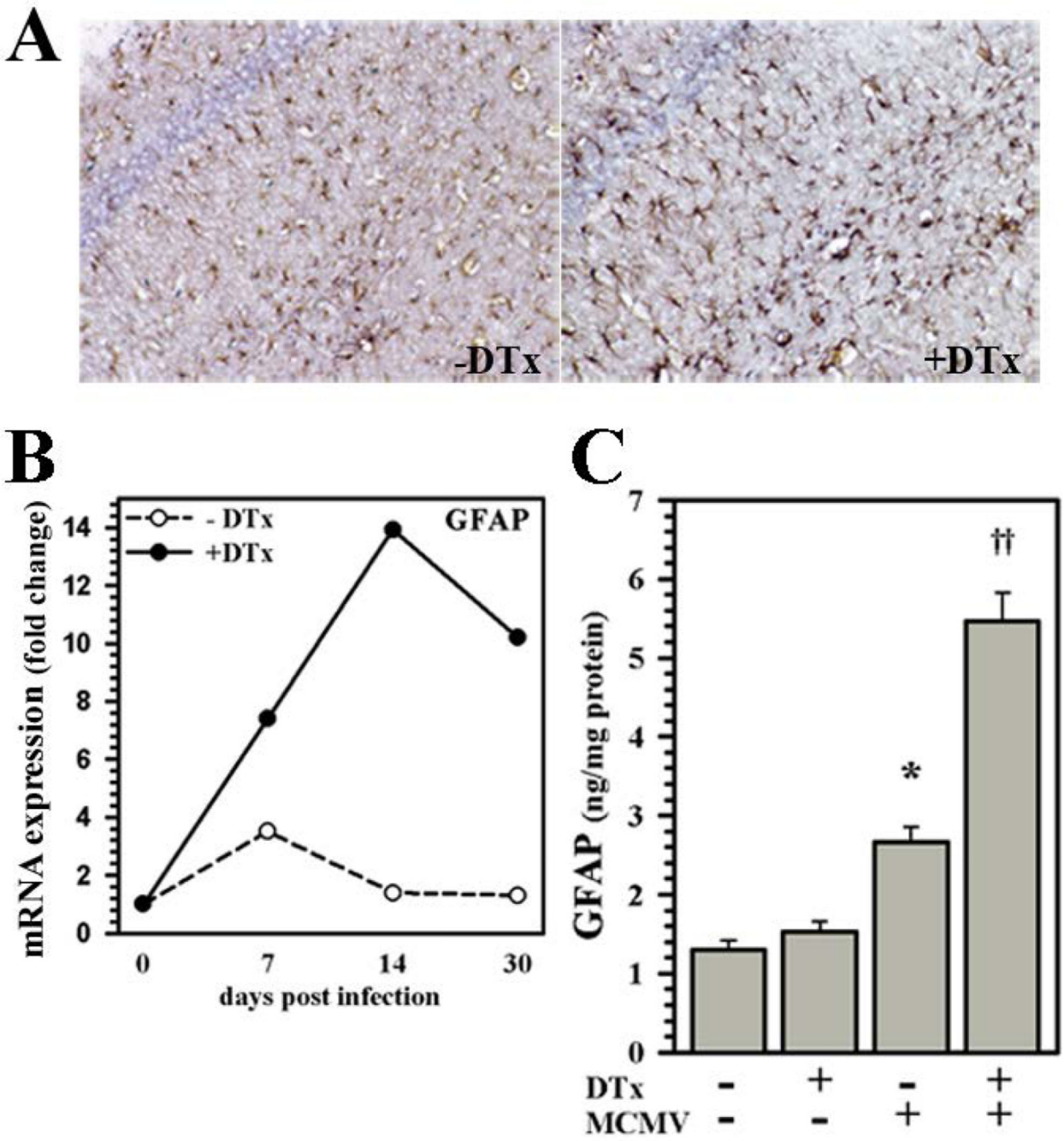

Figure 7. Elevated chronic astrogliosis subsequent to acute Treg depletion

(A) IHC staining of brain sections obtained from MCMV-infected Foxp3-DTR-GFP transgenic mice with (+DTx) or without (−DTx) DTx treatment for expression of GFAP at 40 dpi. **(B)** Brain homogenates were collected from uninfected or untreated and DTx-treated animals; and cDNA was synthesized from 1.0 μg of total RNA. Fold change in GFAP mRNA expression relative to uninfected animals was quantified using the $2^{-\Delta\Delta Ct}$ method and normalized to the housekeeping gene HPRT. Data shown are representative of two experiments using three animals/time point/experiment. **(C)** Differences in GFAP protein

levels in brains with or without infection and Treg depletion (±DTx) were quantified at 40 dpi using ELISA. Pooled data presented are derived from three to nine animals/group. *$P \leq 0.05$ vs. untreated uninfected. $^{\dagger\dagger}P \leq 0.01$ vs. MCMV.

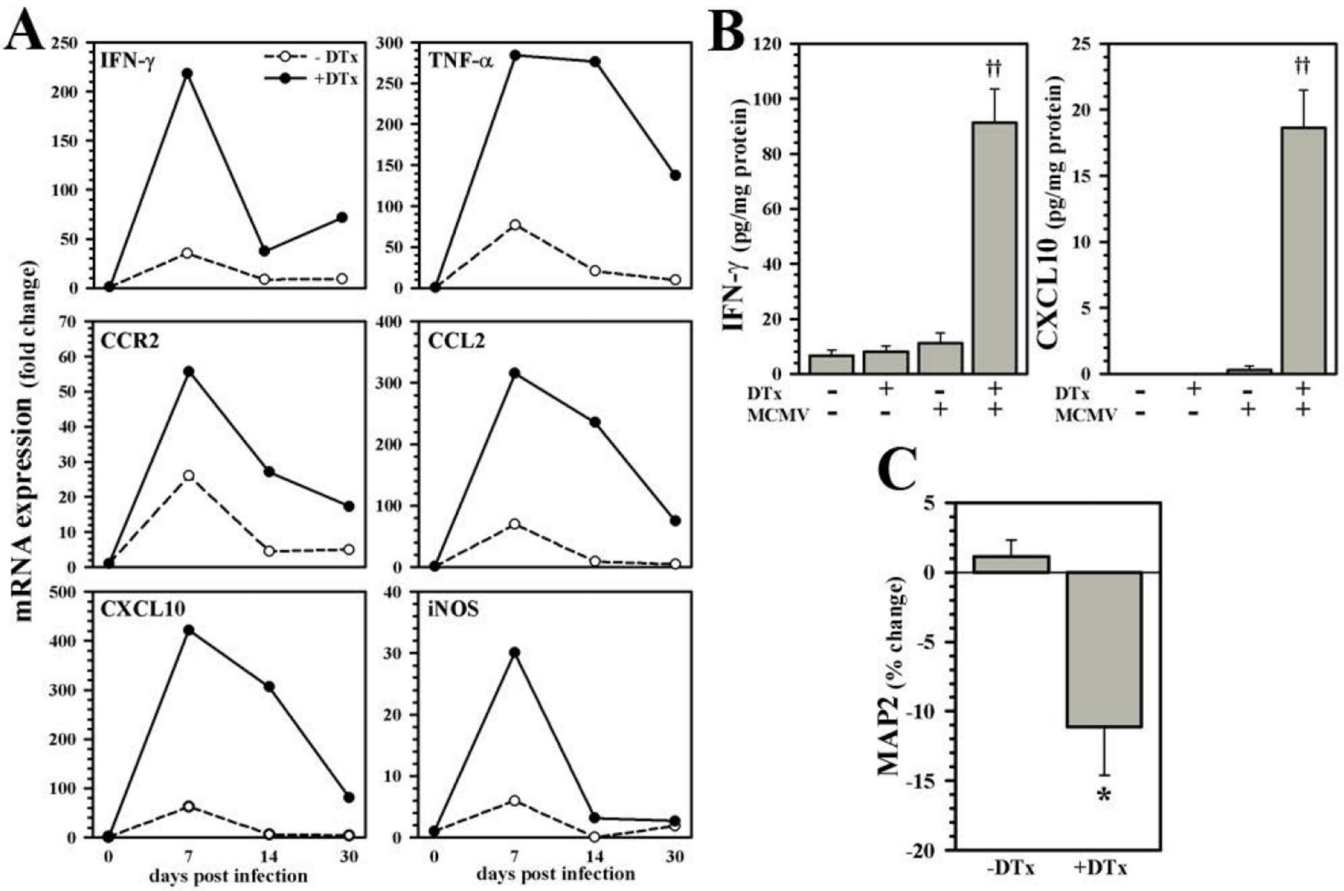

Figure 8. Delayed remission of post-encephalitic neuroinflammation following Treg depletion

(A) Brain tissue homogenates were collected from uninfected or DTx-treated and untreated mice infected with MCMV for expression analysis of the pro-inflammatory mediators IFN-γ, TNF-α, CCR2, CCL2, CXCL10, and inducible nitric oxide synthase (iNOS) at the indicated time points post-infection. Fold change in mRNA levels relative to uninfected animals was quantified using the $2^{-\Delta\Delta Ct}$ method and normalized to the housekeeping gene HPRT. Data shown are representative of two experiments using three animals/time point/experiment. **(B)** Differences in IFN-γ and CXCL10 protein levels in brains with or without infection and Treg depletion (±DTx) were quantified at 40 dpi using ELISA. Data presented are derived from three to nine animals/group. **(C)** Expression of neuronal MAP2 was quantified in infected brains with or without DTx treatment using ELISA at 40 dpi (n = 3 to 9 mice per group). $^{\dagger\dagger}P \leq 0.01$ vs. MCMV. $^{*}P \leq 0.05$ vs. untreated.

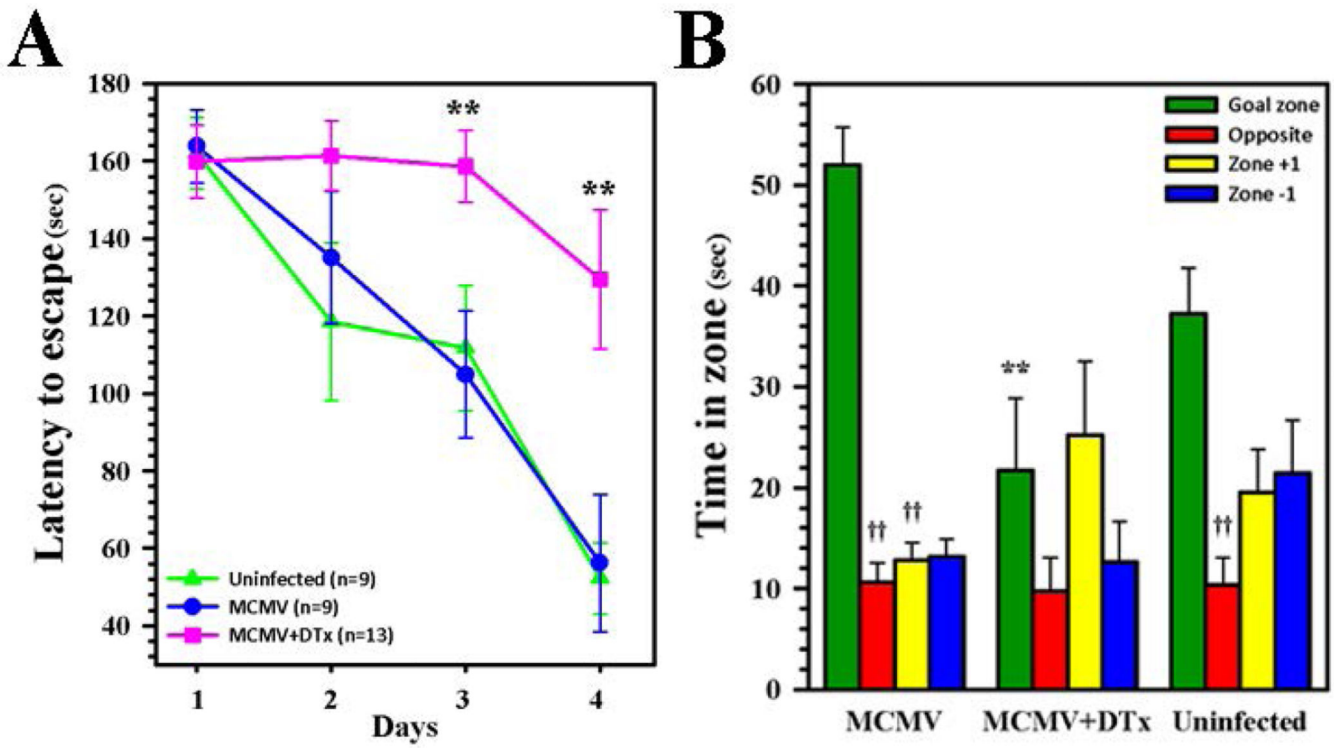

Figure 9. Long-term neurological sequelae following Treg depletion during acute infection

(A) Convalescent Foxp3-DTR-GFP transgenic mice with (MCMV +DTx, pink line, n = 13) and without DTx treatment (MCMV, blue line, n = 9), along with uninfected controls (Uninfected, green line, n = 9), were tested for deficiencies in spatial learning and memory using a Barnes Maze at 30 dpi. The time needed to move to the hole with an escape box on each day of testing was recorded as latency to escape (sec). **(B)** Following 4 d of acquisition using four trials per d (i.e., on d 5), the escape box was covered and the time spent in each quadrant was compared to time spent in the goal zone (90 sec test), which previously contained the escape box. **$P \leq 0.01$ vs. MCMV. $^{\dagger\dagger}P \leq 0.01$ vs. goal zone of each respective group.